

- Supporting Information
- Links to the 13 articles that cite this article, as of the time of this article download
- Access to high resolution figures
- Links to articles and content related to this article
- Copyright permission to reproduce figures and/or text from this article

[View the Full Text HTML](#)



## High-Affinity Binding and Direct Electron Transfer to Solid Metals by the *Shewanella oneidensis* MR-1 Outer Membrane *c*-type Cytochrome OmcA

Yijia Xiong,<sup>†</sup> Liang Shi,<sup>†</sup> Baowei Chen,<sup>†</sup> M. Uljana Mayer,<sup>†</sup> Brian H. Lower,<sup>‡</sup> Yuri Londer,<sup>‡</sup> Saumyaditya Bose,<sup>‡</sup> Michael F. Hochella,<sup>‡</sup> James K. Fredrickson,<sup>†,‡</sup> and Thomas C. Squier<sup>\*†</sup>

Division of Biological Sciences and Environmental Molecular Science Laboratory,  
Biogeochemistry Grand Challenge Program, Pacific Northwest National Laboratory, Richland, Washington 99352

Received May 19, 2006; E-mail: thomas.squier@pnl.gov

The mechanisms by which bacterial outer membrane-associated electron transport proteins interact with extracellular electron acceptors, including Fe and Mn oxides, is poorly understood. The 85 kDa outer membrane decaheme cytochrome OmcA (SO1779) from the dissimilatory metal-reducing bacterium (DMRB) *Shewanella oneidensis* MR-1 can reduce soluble Fe(III) and other metal chelates,<sup>1</sup> and has previously been suggested to function in concert with other membrane proteins as one of the terminal electron donors in the metal reductase protein complex of *Shewanella oneidensis* MR-1.<sup>2</sup> *Shewanella*'s metabolic diversity has considerable promise for the bioremediation of metal and radionuclide contaminants as well as in the design of microbial fuel cells.<sup>3</sup> Biofuel cells offer a potential means to couple the breakdown of biowastes to generate electrical current.<sup>4</sup> Miniaturization of these fuel cells is dependent on the elimination of the membrane between the cathode and anode compartments.<sup>5</sup> It has been demonstrated that the immobilization of redox-active proteins on electrodes renders this membrane unnecessary.<sup>6</sup> The identification of a purified metal-reducing enzyme able to densely bind and directly donate electrons to commonly used iron-oxide-coated electrodes<sup>7</sup> has great potential to contribute to fuel cell design. This will also contribute to understanding how DMRB transfer electrons to solid metal oxides in the environment, which may involve direct interactions with membrane proteins or an indirect mechanism through mineral solubilization or electron shuttling. To identify the terminal electron donors in the *S. oneidensis* metal reductase system and to explore whether isolated proteins can directly bind and mediate electron-transfer reactions to reduce solid metals, we have purified OmcA and measured its ability to bind and transfer electrons to solid Fe<sub>2</sub>O<sub>3</sub> in the mineral hematite.

Hematite nanoparticles were generated using the forced hydrolysis of Fe<sup>3+</sup>(OH)<sub>2</sub> ions to form particles,<sup>8</sup> whose average radius was measured to be 11 ± 2 nm at pH 5 (see Supporting Information). At the physiological pH for the catalytic activity of OmcA (pH 7.5), hematite self-associates to form a broad distribution of size classes ranging from about 10 nm (≈1 particle) to large aggregates with an apparent size of about 400 nm [see Supporting Information (SI) Figure S1]. OmcA directly associates with added hematite, as evidenced by the co-sedimentation of approximately 40% of the OmcA in solution with hematite particles upon centrifugation (Figure 1A), permitting a determination of the binding affinity through the measurement of the concentration of OmcA bound to hematite relative to that in water (i.e., the partition coefficient). We find that approximately 0.2 mg of OmcA binds per mg of hematite (i.e., 2.5 nmol OmcA per mg of hematite). From the average radius of hematite at pH 7.5 (i.e., 400 nm), approximately 10<sup>6</sup> OmcA proteins bind to each particle (i.e., 10<sup>14</sup> OmcA proteins bind per cm<sup>2</sup>), corresponding to a partition

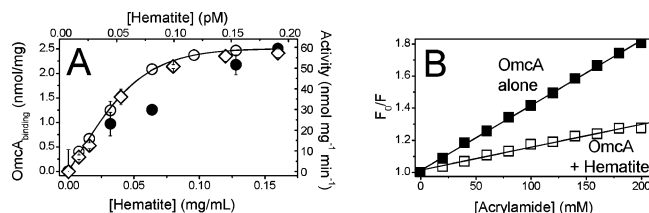


**Figure 1.** Functional association between 1.0  $\mu\text{M}$  OmcA and hematite nanoparticles detected by (A) electron-transfer activity ( $\diamond$ ) or direct binding measured by loss of OmcA through co-sedimentation with hematite particles ( $\circ$ ) following centrifugation (16000g for 10 min) or diminished intrinsic fluorescence ( $\bullet$ ) and (B) decreased solvent accessibility ( $F_0/F$ ) of Trp in OmcA following hematite addition (30  $\mu\text{g}/\text{mL}$ ), where  $F_0/F$  is the fluorescence change upon acrylamide addition.

coefficient of approximately  $2 \times 10^5$  ( $\Delta G^{\circ} = -28$  kJ/mol). A similar high-affinity binding interaction is measured using decreases in the intrinsic tryptophan fluorescence of OmcA to assess binding as a function of added hematite. Furthermore, upon association with hematite there is a large decrease in the solvent accessibility of the tryptophans in OmcA to a soluble acrylamide quencher (Figure 1B), consistent with a direct binding interaction between OmcA and hematite. In contrast, there is no significant binding between OmcA and other minerals or particles (SI Figures S3 and S4), indicating specific binding between OmcA and hematite.

In association with hematite, OmcA is catalytically active: oxidation of protein hemes, as measured from time-dependent changes in the  $\alpha$  Soret absorption peak at 552 nm,<sup>2</sup> directly tracks with protein binding to hematite under anoxic conditions with a maximal activity of about 60 nmol  $\text{mg}^{-1}$  OmcA  $\text{min}^{-1}$ . Since OmcA can be directly reduced by NADH and other metabolic cofactors,<sup>2</sup> the high-affinity interaction between OmcA and hematite provides a means to couple the generation of reducing power to an electrode surface. To confirm the binding specificity, and to detect possible changes in the internal dynamics of OmcA upon association with hematite, we labeled OmcA with the chromophore Alexa-488 and have used fluorescence correlation spectroscopy (FCS) to measure fluorescence intensity fluctuations associated with both changes in internal motion and decreases in the translational diffusion of OmcA upon association with hematite.<sup>9</sup> These measurements utilized a confocal microscope using a pair of SPCM-AQR-14 avalanche photodiodes to perform pseudocross-correlation measurements that efficiently remove after-pulse effects that correspond to spontaneous signals associated with individual photodetectors that can broaden and distort fluorescence intensity traces. The fluorescence intensity trace for Alexa488-labeled OmcA in the absence of hematite is characterized by a high density of low-amplitude bursts, whose frequency is indicative of the concentration of protein in solution (Figures 2A and S5). Upon addition of hematite, there is a dramatic increase in the amplitude (brightness) of some fluorescence bursts that is indicative of multiple OmcA proteins binding to hematite

<sup>†</sup> Division of Biological Sciences.

<sup>‡</sup> Environmental Molecular Science Laboratory.

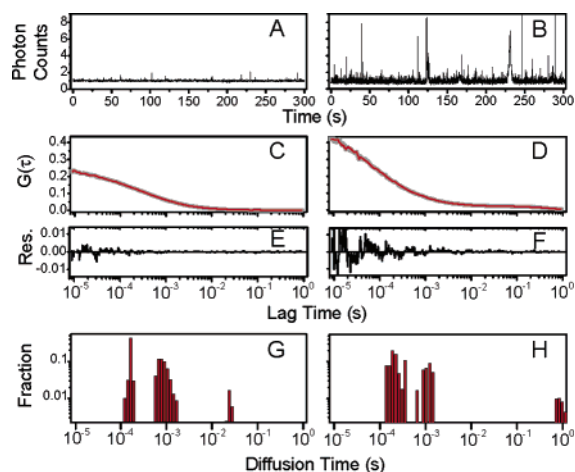


**Figure 2.** Fluorescence intensity traces (A, B) and correlation curves with fits (red) (C, D) for 10 nM Alexa488-labeled OmcA in the absence (left panels) or presence (right panels) of hematite (16  $\mu\text{g}/\text{mL}$ ). Residuals from fits to the correlation data (E, F) and distribution of diffusion times (G, H).

particles (Figure 2B). Other heme-containing proteins do not bind to hematite (SI Figure S6). A quantitative consideration of the sample heterogeneity is possible from a consideration of the fluorescence correlation curves associated with the fluorescence intensity traces (Figure 2, C and D). The correlation curve is described by the equation:

$$G(\tau) = \frac{1}{N} \frac{1}{\left(1 + \frac{\tau}{\tau_D}\right) \cdot \sqrt{1 + \frac{\tau}{S^2 \tau_D}}} \quad \text{where} \quad \tau_D = \frac{\omega^2}{4D_t}$$

$N$  is the number of molecules in the focus point,  $S$  is the ratio of half-height to radius ( $\omega$ ) of the focus point,  $\tau$  is the lag time between fluorescence bursts,  $\tau_D$  is the apparent diffusion time of the molecule, and  $D_t$  is the translational diffusion coefficient. The radius of the focal point ( $\omega$ ) was measured to be 270 nm using both the free dye Alexa488 and a standard fluorescently labeled bead with a known radius ( $r = 50.5$  nm), whose measured translational diffusion time has a narrow distribution centered at 4.73 ms, corresponding to a calculated radius of 52 nm (see SI Figure S2). However, the size of heterogeneous samples cannot be accurately determined by assuming a homogeneous monodisperse solution. Rather, a distribution of diffusion times is described by the following function:

$$f(\tau) = \sum_i A_i G(\tau_i)$$

where  $G(\tau)$  is the FCS curve with diffusion time  $\tau_i$  and  $A_i$  is the fractional amplitude of  $G(\tau)$ . Fits to the correlation function involved modification of the Matlab program Smcontinbot.<sup>10</sup> The small and random residuals indicate that the resulting distribution of diffusion times accurately describe the sample heterogeneity (Figure 2, E and F).

The translational motion of OmcA in the absence of hematite is described by a multimodal distribution of diffusion times centered near 160  $\mu\text{s}$ , 800  $\mu\text{s}$ , and 20 ms (Figure 2G). Using the Stokes–Einstein equation to calculate the hydrodynamic radius (see SI Figure S2), the intermediate diffusion time (i.e.,  $\tau_D = 800$   $\mu\text{s}$ ) with an apparent radius of about 9 nm is consistent with the size of OmcA, which can form a dimer in solution, while the larger diffusion time (i.e.,  $\tau_D = 20$  ms) corresponds to a higher-order oligomer.<sup>2</sup> The smaller diffusion time centered near 160  $\mu\text{s}$  is assigned to internal domain motions that function to modulate the

fluorescence intensity of Alexa488. In the presence of hematite the translational diffusion time for the OmcA dimer is shifted toward a larger time constant (i.e., 1.2 ms), consistent with OmcA molecules binding to small hematite particles (Figure 2H); in addition a larger diffusion time centered near 800 ms is observed that corresponds to the size of hematite particles measured by dynamic light scattering and is associated with approximately  $10^6$  OmcA proteins bound per particle (Figure 1A). Likewise, upon OmcA binding to hematite there is a substantial increase in the relative area associated with OmcA domain motions, which increases from 50 to 70% of the integrated peak area (Figure 2, G and H). Thus, binding to hematite increases domain motions that may facilitate electron-transfer reactions between heme clusters in OmcA by modulating their spatial arrangement.<sup>11</sup>

In summary, we have shown that purified OmcA binds and densely covers the surface of hematite (approximately  $10^{14}$  OmcA proteins bind per  $\text{cm}^2$ ) and reduces Fe(III) with a maximal velocity of approximately 60 nmol/mg/min, which corresponds to an electron flux of about  $10^{13}$  electrons/ $\text{cm}^2/\text{s}$  that approaches observed fluxes in the most efficient bioreactors.<sup>3</sup>

**Acknowledgment.** Supported by Genomics:GTL Program of the Department of Energy (DOE- OBER) and an EMSL Scientific Grand Challenge Project at PNNL, which is operated for DOE by Battelle under Contract DE-AC05-76RL0 1830.

**Supporting Information Available:** Procedures and characterization data; complete refs 2a, 2b, 2c. This material is available free of charge via the Internet at <http://pubs.acs.org>.

## References

- (1) (a) Nealon, K. H.; Saffarini, D. *Annu. Rev. Microbiol.* **1994**, *48*, 311–343. (b) Tiedje, J. M. *Nat. Biotechnol.* **2002**, *20*, 1093–1094. (c) Viamajala, S.; Peyton, B. M.; Apel, W. A.; Petersen, J. N. *Biotechnol. Prog.* **2002**, *18*, 290–295. (d) Viamajala, S.; Peyton, B. M.; Petersen, J. N. *Biotechnol. Bioeng.* **2003**, *83*, 790–797. (e) Wade, R.; DiChristina, T. J. *FEMS Microbiol. Lett.* **2000**, *184*, 143–148.
- (2) (a) Shi, L.; et al. *J. Bacteriol.* **2006**, *188*, 4705–4714. (b) Gorby, Y. A.; et al. *Proc. Natl. Acad. Sci. U.S.A.* **2006**, *103*, 11358–11363. (c) Marshall, M. J.; et al. *PLoS Biol.* **2006**, *4*, 1324–1333. (d) Wigginton, N. S.; Rosso, K. M.; Lower, B. H.; Shi, L.; Hochella, M. F., Jr. *Geochim. Cosmochim. Acta* **2006**. In press.
- (3) (a) Viamajala, S.; Peyton, B. M.; Apel, W. A.; Petersen, J. N., *Biotechnol. Bioeng.* **2002**, *78*, 770–778. (b) Ringelsen, B. R.; Henderson, E.; Wu, P. K.; Pietron, J.; Ray, R.; Little, B.; Biffinger, J. C.; Jones-Meehan, J. M. *Environ. Sci. Technol.* **2006**, *40*, 2629–2634.
- (4) (a) Bond, D. R.; Lovley, D. R. *Appl. Environ. Microbiol.* **2003**, *69*, 1548–1555. (b) Kim, B. H.; Park, H. S.; Kim, H. J.; Kim, G. T.; Chang, I. S.; Lee, J.; Phung, N. T. *Appl. Microbiol. Biotechnol.* **2004**, *63*, 672–681. (c) Liu, H.; Ramnarayanan, R.; Logan, B. E. *Environ. Sci. Technol.* **2004**, *38*, 2281–2285.
- (5) Kim, H.-H.; Mano, N.; Zhang, Y.; Heller, A. *J. Electrochem. Soc.* **2003**, *150*, A209–A213.
- (6) (a) Chen, T.; Barton, S. C.; Binyamin, G.; Gao, Z.; Zhang, Y.; Kim, H. H.; Heller, A. *J. Am. Chem. Soc.* **2001**, *123*, 8630–8631. (b) Mano, N.; Kim, H. H.; Zhang, Y.; Heller, A. *J. Am. Chem. Soc.* **2002**, *124*, 6480–6486. (c) Mano, N.; Mao, F.; Heller, A. *J. Am. Chem. Soc.* **2002**, *124*, 12962–12963. (d) Mano, N.; Mao, F.; Heller, A. *J. Am. Chem. Soc.* **2003**, *125*, 6588–6594. (e) Mano, N.; Mao, F.; Heller, A. *ChemBioChem* **2004**, *5*, 1703–1705. (f) Mano, N.; Mao, F.; Shin, W.; Chen, T.; Heller, A. *Chem. Commun. (Camb)* **2003**, 518–519. (g) Soukharev, V.; Mano, N.; Heller, A. *J. Am. Chem. Soc.* **2004**, *126*, 8368–8369.
- (7) Kim, J. R.; Min, B.; Logan, B. E. *Appl. Microbiol. Biotechnol.* **2005**, *68*, 23–30.
- (8) Madden, A. S.; Hochella, M. F., Jr.; Michael, F. *Geochim. Cosmochim. Acta* **2005**, *69*, 389–398.
- (9) (a) Chattopadhyay, K.; Saffarian, S.; Elson, E. L.; Frieden, C. *Proc. Natl. Acad. Sci. U.S.A.* **2002**, *99*, 14171–14176. (b) Haupts, U.; Maiti, S.; Schwill, P.; Webb, W. W. *Proc. Natl. Acad. Sci. U.S.A.* **1998**, *95*, 13573–13578. (c) Miguel Angel Medina, P. S. *BioEssays* **2002**, *24*, 758–764. (d) R. Rigler, E. S. E. *Fluorescence correlation spectroscopy, theory and application*; Springer: New York, 2001. (e) Whittier, J. E.; Xiong, Y.; Rechsteiner, M. C.; Squier, T. C. *J. Biol. Chem.* **2004**, *279*, 46135–46142.
- (10) (a) Smcontinbot at <http://www.mathworks.com/matlabcentral/fileexchange/loadCategory.do>. (b) Provencher, S. W. *Comput. Phys. Commun.* **1982**, *27*, 213–27.
- (11) (a) Smith, D. M.; Rosso, K. M.; Dupuis, M.; Valiev, M.; Straatsma, T. P. *J. Phys. Chem. B* **2006**, *110*, 15582–15588. (b) Scrutton, N. S. *Biochem. Soc. Trans.* **1999**, *27*, 767–779.

JA063526D